Nondestructive testing and crack evaluation of ferromagnetic material by using the linearly integrated hall sensor array [†]

Jinyi Lee[1,*], Jiseong Hwang[2], Jongwoo Jun[2] and Seho Choi[3]

[1]Department of Control Instrumentation and Robot Engineering, Chosun University,
375, Seosuk-dong, Dong-gu, Gwangju, 501-759, Republic of Korea
[2]Department of Information and Communication Engineering, Graduate School of Chosun University,
375, Seosuk-dong, Dong-gu, Gwangju, 501-759, Republic of Korea
[3]Technical Research Laboratory, Instrumentation and Control Research Group, POSCO
1 Goedong-dong, Nam-gu, Pohang, Gyengbuk, 790-785, Republic of Korea

───

Abstract

Magnetic flux leakage testing (MFLT), which measures the distribution of a magnetic field on a magnetized specimen by using a magnetic sensor such as a Hall sensor, is an effective nondestructive testing (NDT) method for detecting surface cracks on magnetized ferromagnetic materials. A scan-type magnetic camera, based on the principle of MFLT, uses an inclined Hall sensor array on a printed circuit board (PCB) to detect small cracks at high speed. However, the wave forms appear in a direction perpendicular to the scan because the sensors are bonded at different gradients and heights on the PCB despite careful soldering. In this paper, we propose linearly integrated Hall sensors (LIHaS) on a wafer to minimize these waves and to improve the probability of crack detection. A billet specimen is used to determine the effectiveness of the LIHaS in multiple crack detection.

Keywords: Magnetic camera; Sensor array; Ferromagnetic; Crack; NDT

───

1. Introduction

A digital camera consists of a light source, object, optical lens, 1- or 2-dimensional arrayed optical sensors, an analog-to-digital converter (ADC), an interface, a processor, and a display. The light flux from the light source is reflected, absorbed, and diffused on the surface of the object according to the object type, color, and shape. The distribution of the optical intensity is affected by these optical phenomena in space. After which, the changed light flux distribution, passing through an optical lens, is collected in an optical sensors array, such as a CCD sensor. The distribution of optical intensity is converted to a distribution of the

digitized electrical value array by an ADC. Therefore, the distribution of the optical intensity can be stored, processed and observed by using the interface, a processor, and a display.

On the other hand, Lee et al. reported a magnetic camera able to visualize the distribution of the magnetic field [1-9]. A magnetic camera can be used in nondestructive testing and estimation of metal in hidden areas [2, 4, 5]. A magnetic camera consists of a magnetic source, object, magnetic lens, 1- or 2-dimensional arrayed magnetic sensors, an ADC, an interface, a processor, and a display. The electromagnetic coil, the Helmholtz coil, a solenoid, and a sheet type induced current can be used as a magnetic source. The induced magnetic field can be distorted by the existence of objects in space or cracks in the specimen. Therefore, the distribution of the magnetic field intensity can be changed. The changed magnetic flux

can be concentrated on the magnetic lens [2, 3, 5-7, 9], thereby enabling the distribution of the electrical signal array to be changed by using arrayed magnetic sensors, such as Hall sensors, and an ADC. In addition, the shape of the material and the cracks in the specimen can be analyzed quantitatively. In this paper, we consider a scan-type magnetic camera [1, 6], with the Hall sensors arrayed perpendicular to the scanning direction on the specimen. In a previous work [6], the scan-type magnetic camera had limitations in spatial resolution and the extension of image processing due to the usage of packaged Hall sensors. We propose a linearly integrated Hall sensor array (LIHaS) on a wafer, with sensors bonded at different gradients and heights on a PCB, to minimize the waves. We used a billet specimen to determine the LIHaS effectiveness in the detection of multiple cracks.

2. Problem definition

A magnetic camera, able to measure the distribution of a magnetic field (DMF) by using the Hall sensor array on the magnetized specimen, has been applied in detecting and evaluating cracks on ferromagnetic specimens. The spatial resolution in the matrix-type Hall sensor array is lowered as a necessary consequence due to the packaged size and the sensor pins [6]. However, the matrix-type Hall sensor array is not needed in a continuous process.

Fig. 1(a) shows the array method for the packaged Hall sensors to obtain a high spatial resolution of 1mm for a specimen moving perpendicular to the sensor lines [6]. Sometimes, the Hall sensor array is scanned on the specimen by using the high precision movement equipment shown in Fig. 1(b). The packaged Hall sensors are carefully located on the PCB, but differences come about in the lift-off and gradient among the sensors. Therefore, the DMF signals from the Hall sensor array on a PCB are significantly different than the DMF signals obtained by using single Hall sensor scanning. To explain the limitations of the previous Hall sensor array method and to propose an improved method, we introduced holes and slits on the high-carbon steel billet specimens (SCM435, 132×125.5×20 mm) by using electrical discharge machining as shown in Fig. 2 and Table 1.

We inputted a direct current of 700mA to the yoke-type magnetizer (250 mm of the pole distance, number of winding is 4,000 turns). The lift-off was 1.2 mm. Fig. 3 shows the distribution of Hall voltages

Table 1. Crack sizes on each specimen.

Shape	Crack size, [mm]			Volume, [mm³]
	Radius	Depth	Width	(A_{CROSS}, [mm²])
Hole type	0.25	0.4		0.08 (0.2)
		1.0		0.19 (0.5)
		1.5		0.29 (0.75)
	0.5	0.4		0.31 (0.4)
		1.0		0.79 (1)
		1.5		1.17 (1.5)
	1	0.4		1.25 (0.8)
		1.0		3.14 (2)
		1.5		4.71 (3)
	1.5	0.4		2.83 (1.2)
		1.0		7.06 (3)
		1.5		10.60 (4.5)
	2.5	0.4		7.85 (2)
		1.0		19.63 (5)
		1.5		29.45 (7.5)

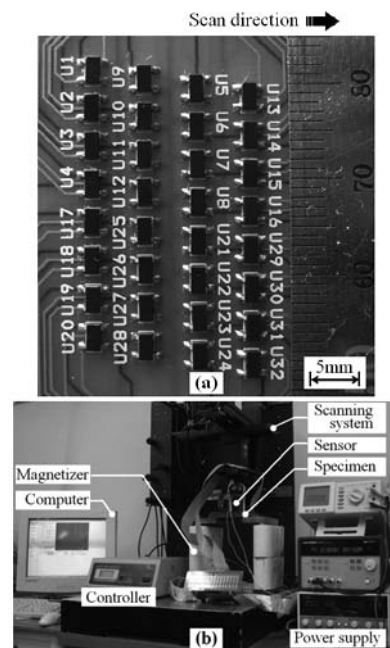| Shape	Crack size, [mm]			Volume, [mm³]
	Length	Depth	Width	(A_{CROSS}, [mm²])
Slit type 0°, 45°, 90°	5	0.2	0.2	0.2 (0.04,0.71,1)
			0.4	0.4 (0.08,0.71,1)
			1.0	1.0 (0.20,0.71,1)
	10	0.4	0.2	0.8 (0.08,2.83,4)
			0.4	1.6 (0.16,2.83,4)
			1.0	4.0 (0.40,2.83,4)
	15	0.6	0.2	1.8 (0.12,6.36,9)
		1.0	0.4	6 (0.4,10.61,15)
			1.0	15 (1.0,10.61,15)

Fig. 1. Components of a scan-type magnetic camera: (a) inclined Hall sensors array, and (b) high precision scanning system.
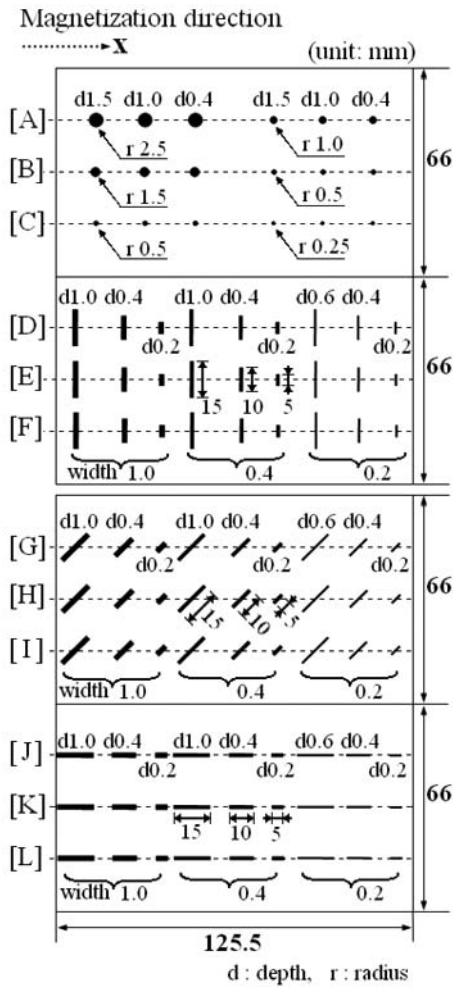
Fig. 2. Schematic graphs of cracks on each specimen.

Fig. 3. Magnetic camera images using arrayed sensors on a PCB: (a) V_H, distribution of Hall voltages, (b) $\partial V_H / \partial x$ image, and (c) $\partial V_H / \partial y$ image.

(V_H image), measured by using the sensor array illustrated in Fig. 1(a) and the scanning system of Fig. 1(b). The distribution of the differential V_H image, parallel to the scanning direction (x-direction), is hereafter expressed as a $\partial V_H / \partial x$ image. That distribution, perpendicular to the scanning direction (the y-direction) is hereafter expressed as a $\partial V_H / \partial y$ image, respectively. The small waves in the y-direction are shown in the V_H image, despite the precise magnetic-to-electric calibration of each sensor [6]. In addition, the large inclined distribution of V_H due to the magnetizer poles, is shown in the V_H image. The small variation of V_H due to the crack existence appearing around a crack cannot be distinguished because of the large magnetic gradient, as shown in Fig. 3(a). However, the magnetic gradient, due to the magnetizer, is approximately homogeneous enabling the crack to be
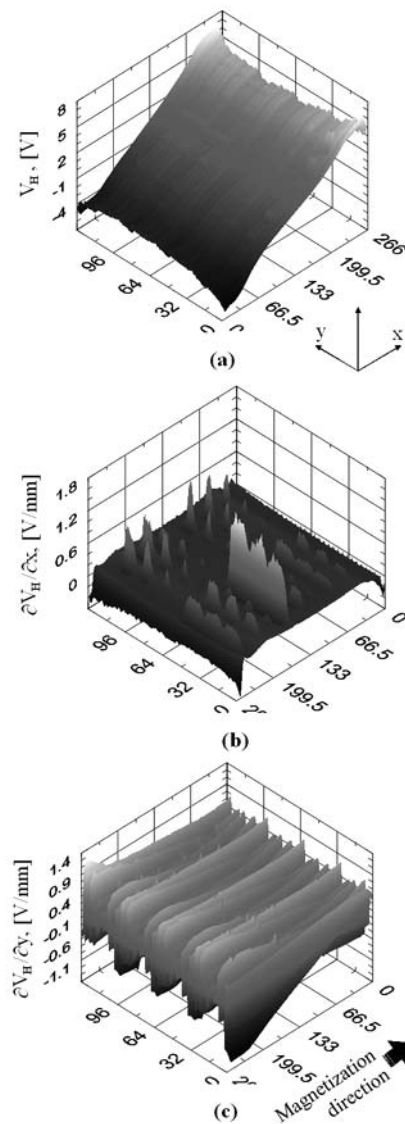
detected in the $\partial V_H / \partial x$ image as shown in Fig. 3(b). The crack cannot be visualized in the $\partial V_H / \partial y$ image, as shown in Fig. 3(c), because of the aforementioned appearance of small waves in the y-direction of the V_H image.

Fig. 4 shows the 3-dimensional displacements on the PCB, obtained by using a laser displacement sensor between the base plane and the sensors array, as shown in Fig. 1(a). The small waves of Fig. 3(a) are due to the variation of the displacement and gradients of each sensor, as shown in Fig. 4.
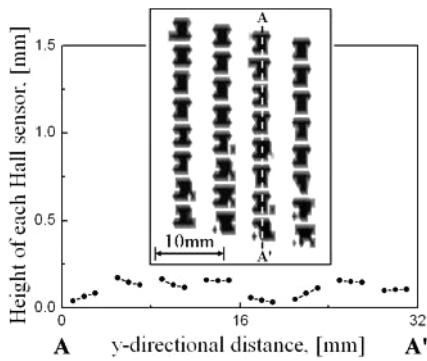
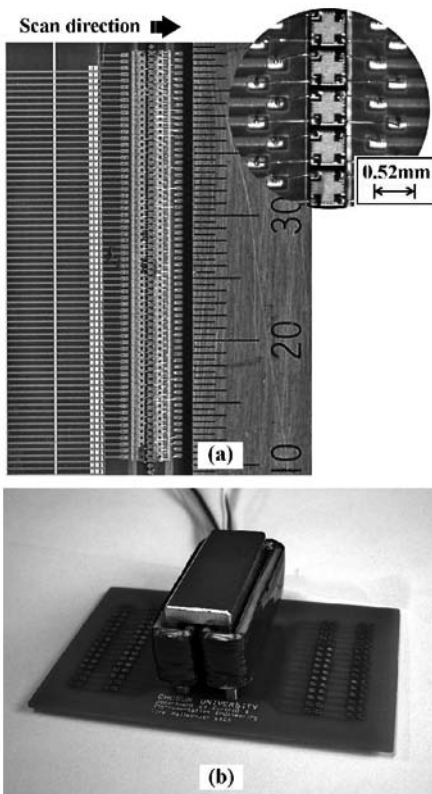Fig. 4. Scan result of sensors array using a 3D laser displacement sensor.

Fig. 5. Photograph of the linearly integrated Hall sensors (LIHaS): (a) 64 InSb Hall sensors, and (b) small yoke-type magnetizer.

3. Experiments and solutions

The 64 InSb Hall sensors are linearly integrated on the Ni-Zn ferrite wafer with 0.52 mm spatial resolution, as shown in Fig. 5(a). They are used to obtain the V_H image. The gradients and the displacement variation are minimized by using a LIHaS. In addition,
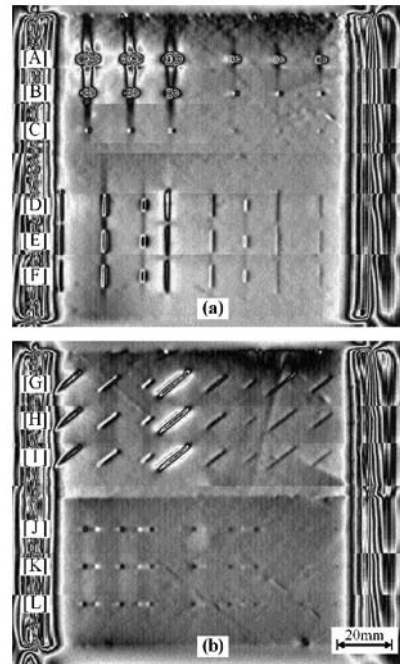

Fig. 6. Result of $\partial V_H/\partial x$ of LIHaS: (a) specimen of Fig. 2(a), and (b) specimen of Fig. 2(b).
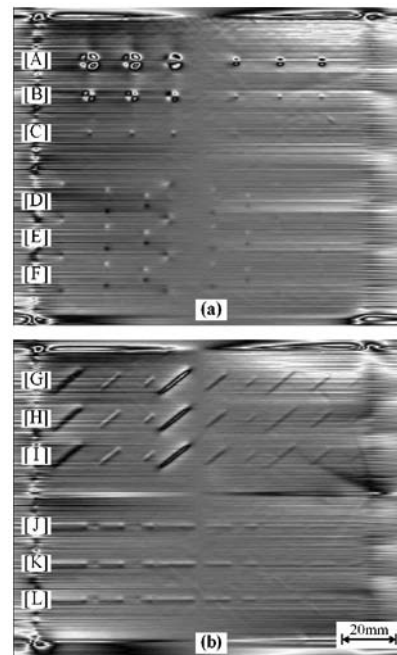

Fig. 7. Result of $\partial V_H/\partial y$ of LIHaS: (a) specimen of Fig. 2(a), and (b) specimen of Fig. 2(b).

the high spatial resolution permits the arrangement of the sensor array in a smaller area than the case illustrated in Fig. 1(a). We obtain the $\partial V_H/\partial x$ (Fig. 6) and

$\partial V_H/\partial y$ (Fig. 7) images by processing the V_H image measured on the specimen shown in Fig. 2. The specimen was magnetized by using a small yoke-type magnetizer (magnetizer), which was positioned back on the LIHaS, as shown in Fig. 5(b). The pole interval of the magnetizer was 12 mm. We inputted a 250 mA direct current to the 1110 turns of the magnetizer coil. The lift-off was 0.5 mm.

The hole-type cracks are distinguished in the $\partial V_H/\partial x$ image, as shown in the top of Fig. 6(a), [A][B][C]. The smallest crack, with a radius of 0.25 mm and a depth of 0.4 mm, was detected by using a LIHaS. The slit-type cracks were detected in the $\partial V_H/\partial x$ image when the angle between the magnetic flux direction and the crack length direction (θ_{MAG}) was 90° (the bottom of Fig. 6(a), [D][E][F]) and 45° (the top of Fig. 6(b), [G][H][I]), respectively. Furthermore, in the bottom of Fig. 6(b), [J][K][L], the image of $\partial V_H/\partial x$ alternates between bright and dark when θ_{MAG} was 0°. These cracks could not be detected by using the previous array method as indicated in Fig. 1. As result, the probability of crack detection improved by using LIHaS. Conversely, the hole-type at Fig. 6(a) and the slit-type with θ_{MAG} of 0° were similar and difficult to distinguish.

Hole-type cracks and slit-type cracks can be detected by using the $\partial V_H/\partial y$ image, as shown in the top of both Figs. 7(a) and (b), respectively. In Fig. 3(c), the cracks cannot be detected by $\partial V_H/\partial y$, whereas the improved LIHaS technology can detect cracks in the $\partial V_H/\partial y$ image. The hole-type cracks can be distinguished from slit-type cracks in the $\partial V_H/\partial y$ image, as shown in the top of Fig. 7(a). That is, the $\partial V_H/\partial x$ image around the hole-type crack, as shown in Fig. 6(a), [A][B][C] was similar to the $\partial V_H/\partial x$ image around the slit-type crack of θ_{MAG} of 0°, as shown in Fig. 6(b), [J][K][L]. Nevertheless, the shape and length could be distinguished by using the $\partial V_H/\partial y$ image. From these results, the shape, θ_{MAG} and crack length directions can be determined from the LIHaS in the $\partial V_H/\partial x$ and $\partial V_H/\partial y$ images.

Fig. 8 shows the 1-dimensional $\partial V_H/\partial x$ distribution on the center lines of each crack. The maximum and minimum of $\partial V_H/\partial x$ (Max[$\partial V_H/\partial x$], Min[$\partial V_H/\partial x$]) around each crack increase with increasing crack size. However, irrespective of the real crack information, a large Max[$\partial V_H/\partial x$] is shown on the specimen edge. Also, Max[$\partial V_H/\partial x$] is minimized if and only if θ_{MAG} equals 0°. Furthermore, with increasing crack length, not only Max[$\partial V_H/\partial x$] and Min[$\partial V_H/\partial x$], but also the
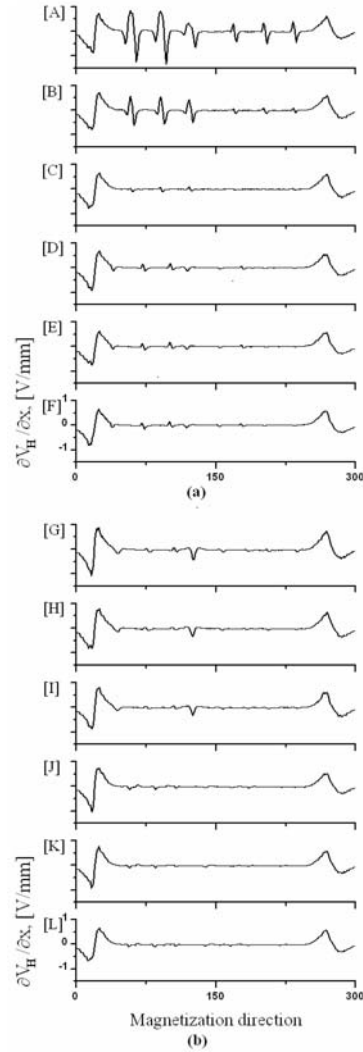

Fig. 8. Section views of $\partial V_H/\partial x$ image: (a) specimen of Fig. 2 (a), and (b) specimen of Fig. 2(b).

distance between Max[$\partial V_H/\partial x$] and Min[$\partial V_H/\partial x$] increases because the crack length affects the $\partial V_H/\partial x$ distribution. Correspondingly, we introduce a weighting method, using length information, in this paper. If the crack length, L_c on the $\partial V_H/\partial x$ image, is more than double the spatial resolution, S (0.5 mm), the crack volume information, $\partial V_H/\partial x|_{total}$, is calculated by using the following equation:

$$\left.\frac{\partial V_H}{\partial x}\right|_{total} = \sum_{i=1}^{L_c/S}\left[Max\left(\frac{\partial V_{H,i}}{\partial x}\right) + Abs\left(Min\left(\frac{\partial V_{H,i}}{\partial x}\right)\right)\right]$$
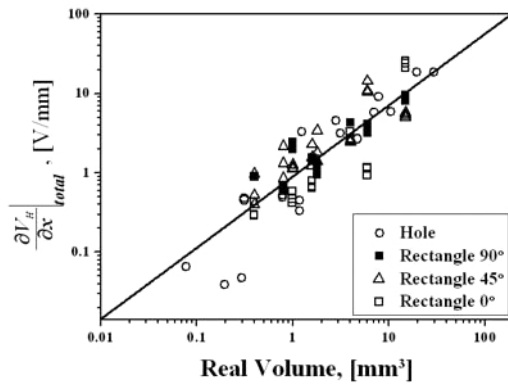
(1)

Fig. 9. Relationships between real crack volume and $\partial V_H/\partial x|_{total}$.

$\partial V_H/\partial x|_{total}$ for the case of L_c being used in Eq. (1). We obtained a linear algebraic equation to evaluate the crack volume:

$$V_c = 1.13934 \cdot \left(\frac{\partial V_H}{\partial x}\bigg|_{total} \right)^{1.112384} \tag{2}$$

where V_c is calculated volume of the crack.

We propose an algorithm for evaluating a crack using the above-mentioned test results as shown in Fig. 10. The spatial resolution of scanning, S, is determined according to the equipment shown in Fig. 1(b). In addition, the operator has to determine the detectable crack length, L, by using a LIHaS. Next, V_H, $\partial V_H/\partial x$ and $\partial V_H/\partial y$ images are obtained by using a scan-type magnetic camera. The length (L_c), angle (θ_{MAG}) between the magnetization direction and the crack length direction, and the crack shape are estimated by using the $\partial V_H/\partial x$ and $\partial V_H/\partial y$ images shown in Fig. 6 and Fig. 7. If L_c is larger than L, then L_c/S is determined by using the $\partial V_H/\partial x$ image, or is assigned a value of 1 as in the other cases. The crack volume information $\partial V_H/\partial x|_{total}$ can be calculated by using Eqs. (1) and (2). Therefore, the crack shape, length, direction, and volume can be evaluated by using the proposed algorithm and the LIHaS system.

4. Conclusions

In this paper, we proposed a linearly integrated, 64 InSb LIHaS on a Ni-Zn ferrite wafer with a spatial resolution of 0.52 mm in order to minimize the height differences and the gradient of each sensor on a PCB. The distribution of Hall voltages, representing the distribution of the magnetic field intensity on the magnetized specimen, was measured by using a LIHaS. Cracks were detected by using two processed images: $\partial V_H/\partial x$ and $\partial V_H/\partial y$. The smallest detected crack was a hole-type with a radius of 0.25 mm and a depth of 0.4 mm. The crack shape, length and direction were estimated by using $\partial V_H/\partial x$ and $\partial V_H/\partial y$ images. Finally, the crack volume was successfully evaluated by using the proposed equation and a new and unique algorithm.

Acknowledgment

ation algorithm.

$_i/\partial x$] and Min[$\partial V_{H,i}/\partial x$] express the values on the $\partial V_H/\partial x$ image around ively. Fig. 9 shows the relationship l volume of the crack and the
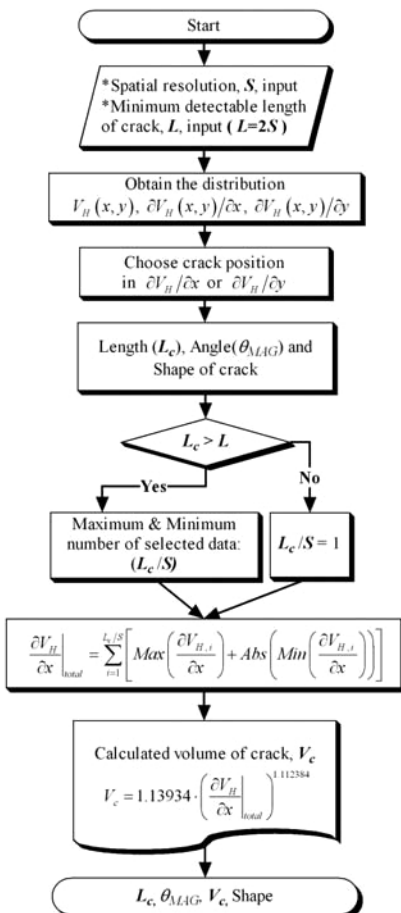
10029-0).

References

[1] J. S. Hwang and J. Y. Lee, Modeling of a scan type magnetic camera image using the improved dipole model, *J. Mech. Sci. Technol.,* 20 (10) (2006) 1691-1701.

[2] J. Y. Lee, et al., A display apparatus of magnetic flux density using 2-D array magnetic sensor and 3-D magnetic fluid, International Application Published Under the Patent Cooperation Treaty (2002) WO 02/08745.

[3] J. Y. Lee, et al., Numerical consideration of lens of magnetic camera for quantitative nondestructive evaluation, *Key Engineering Materials,* 270-273 (2004) 630-635.

[4] J. Y. Lee, et al., Development of magnetic camera using 2-D arrayed hall elements, Proc. APCFS & ATEM'01 (2004) 222-227.

[5] J. Y. Lee, et al., Magnetic flux density apparatus for, E.G., Detecting an internal crack of a metal or a shape of the metal, US patents (2004) 6,683,452 B2.

[6] J. Y. Lee, et al., A study of leakage magnetic flux detector using Hall sensors array, *Key Engineering Materials,* 306-308 (2006) 235-240.

[7] J. Y. Lee, et al., Detection probability improvement for nondestructive evaluation using a magnetic camera, *Key Engineering Materials,* 306-308 (2006) 241-246.

[8] J. Y. Lee, et al., The QNDE using image processing of the magnetic camera, Int. *J. Mod. Phys.,* B 20 (25-27) (2006) 4625-4630.

[9] J. Y. Lee and J. Hwang, The detection probability improvement of the far-side crack on the high lift-off using the magnetic camera, Int. *J. Mod. Phys.,* B 20 (25-27) (2006) 4631-4636.

Prof. Jinyi Lee was born in Korea in 1968. He received the bachelor degree in mechanical design from Chonbuk University, Jeonju, Korea, in 1992. Also he received the master and Ph.D degree in mechanical and aeronautics & space engineering from Tohoku university, Sendai, Japan, in 1995 and 1998, respectively.

He was a Researcher from 1998 to 2000 with the Tohoku university, Iwate university, Iwate Techno-Foundation and Saitama university, Japan. From 2000 to 2003, he worked for Lacomm Co., Ltd. and Gloria Techniques, Korea, as a researcher. In 2003, he was a lecturer with the Chosun university, Gwangju, Korea. Since 2005, he has been an Assistance Professor, Chosun university. His research interests are in application of magneto-optical film, laser and CCD line scan sensor, and development of magnetic camera. He is the author or coauthor of fifteen patents and over 50 scientific papers.

Jiseong Hwang was born in Republic of Korea in 1979. He received the B.S and M.S degree in control and instrumentation engineering in 2005 and 2006, respectively, from the Chosun University, Gwangju, korea, where he is currently working toward the Ph.D. degree.

His research interests are NDT and Evaluation, Magnetic camera.

Jongwoo Jun was born in Korea in 1974. He received the bachelor degree in electronics engineering from Inje University, Kimhae, Korea, in 1999. He received the master degree in electronics engineering from Changwon University, Changwon, Korea, in 2005. Also he is currently working toward the Ph.D. degree in information & communication engineering from Chosun University, Gwangju, Korea.

He worked for Lacomm Co., Ltd. and Gloria Techniques from 1999 to 2005, Korea, as a researcher. His research interests are development of magnetic camera, NDT and evaluation.

Dr. Seho Choi was born in Korea in 1964. He received bachelor degree in the department of electrical and electronic engineering from Kyungpook National University, Daegu, Korea, in 1987. And he received master degree in the department of elec-

trical and electronic engineering from Korea Advanced Institute of Science and Technology in 1989. He received Ph.D. degree in the department of electrical and electronic engineering from the University of Sheffield in the U.K. in 2001.

He had been worked for Agency for Defense Development as a Researcher from 1989 to 1992, Korea. Since 1993, he has been worked for POSCO Research Lab. as a principal researcher. His main research activities are developing Surface Defect Inspection System for hot and cold rolled steel strip, hot wire rod, and hot slab. He is also interested in developing Internal Defect Detection System for steel products by using Ultra-sonic and magnetic camera techniques. His major is image processing to detect tiny defect in high background noise image. He published many scientific papers as the author or co-author.